https://doi.org/10.21289/KSIC.2022.25.2.141

Comparison of Threshold Stress Intensity Factor and Fatigue Limit for Micro-crack of Offshore Structural Steel F690

Kyoung-Hee Gu[1], Gum-Hwa Lee[1], Weon-Gu Lee[2],
Chang-Seok Oh[2], Ki-Woo Nam[1,3*]

〈Abstract〉

In this paper, the evaluation equations proposed by Tange et al. and Ando et al. were used to evaluate the threshold stress intensity factor $\Delta K_{th(s)}^{R}$ and fatigue limit $\Delta\sigma_{wc}^{R}$, according to the small crack of offshore structural steel F690. Despite the differences in concept and shape of the two equations, the $\Delta K_{th(s)}^{R}$ and $\Delta\sigma_{wc}^{R}$ proved completely consistent. It is possible to use these equations to evaluate the dependence of the crack length on the $\Delta K_{th(s)}^{R}$ and $\Delta\sigma_{wc}^{R}$ of structures made of all steel grades. With these equations, the characteristics of microcracks can be quantitatively evaluated, and the safety and reliability of the structure can be secured.

Keywords : Equivalent Crack, Fatigue Limit, Micro Crack, Semi-Elliptical Crack, Threshold Stress Intensity Factor

1 Graduate student, Dept. Marine Convergence Design Engineering, Pukyong National University, Busan, Korea
2 Graduate student, Dept. Materials Science and Engineering, Pukyong National University, Busan, Korea
3* Professor, Dept. Materials Science and Engineering, Pukyong National University, Busan, Korea
E-mail: namkw@pknu.ac.kr

1. Introduction

Generally, the safety of fracture is ensured when the applied stress on the structure satisfies a certain limit. The limit value is determined by the material properties. Material properties are obtained from the material strength test without cracks or defects. However, most of the actual structures contain, or are likely to cause, cracks. As a result, fracture occurs, even under stresses less than the yield strength or tensile strength. Fracture mechanics predicts the fracture behavior and safety based on the dynamic relationship of the crack tip using continuum mechanics, under the premise that cracks exist in the structure. Fracture mechanics quantitatively determines how dangerous a crack is, and how it will grow, dependent on the existing cracks or the environment, and the loads in which the cracks are probabilistically expected to exist [1-9].

In particular, linear fracture mechanics requires that the plastic or nonlinear region occurring at the crack tip be very small, compared to the crack length. The stress intensity factor (K) [10-12] of linear fracture mechanics depends on the fracture toughness of metals and ceramics, and the threshold stress intensity factor of fatigue crack propagation [13]. However in small cracks, as the crack length increases, these values increase; but above a certain crack length, the values become constant, regardless of the crack length. Therefore, the fracture of the structure will depend on how the microcrack problem is controlled. El Haddad et al [14]. proposed a threshold stress intensity factor that depends on the microcrack length, while Tange et al.[15] proposed a modification of the El Haddad equation. Ando et al.[16] proposed an equation for evaluating the threshold stress intensity factor in consideration of the plastic region size by the Dugdale model [17]. Using this equation, the reliability improvement of F690[18] and the fatigue limit of SCM435[19] for microcracks were studied.

In this study, we evaluated the threshold stress intensity factor (ΔK_{th}^{R}) and the fatigue limit (σ_{wc}^{R}) according to the microcrack length in offshore structural steel F690 using the equations proposed by Tange[15] and Ando[16], which can be unified to evaluate the microcrack problems.

2. Evaluation Method

The threshold stress intensity factor range ($\Delta K_{th(s)}^{R}$) of the fatigue crack growth of the small crack in the material can be obtained from Eq. (1):

$$\Delta K_{th(s)}^{R} = \Delta\sigma_{wc}^{R}\sqrt{\pi l} \tag{1}$$

Equation (2) can be used to evaluate the crack length dependence of the threshold stress intensity factor range ($\Delta K_{th(s)}^{R}$) of a small crack as a function of the crack length

(l), the fatigue limit of a smooth specimen ($\Delta\sigma_w^R = 740\text{MPa}$), and the threshold stress intensity factor range ($\Delta K_{th(l)}^R = 6.51\text{MPa}\sqrt{m}$) of a large crack[16]:

$$\Delta K_{th(s)}^R = 2\Delta\sigma_w^R\sqrt{\frac{l}{\pi}}\cos^{-1}\left[\left\{\frac{\pi}{8l}\left(\frac{\Delta K_{th(l)}^R}{\Delta\sigma_w^R}\right)^2+1\right\}^{-1}\right] \quad (2)$$

Meanwhile, Tange et al. obtained Eq. (3) by removing l_0 from the El Haddad equation[15]:

$$\Delta K_{\text{th(s)}}^R = \Delta\sigma_{\text{wl}}^R\sqrt{\pi l} = \frac{\Delta K_{\text{th(l)}}^R\sqrt{l}}{\left\{l+\frac{1}{\pi}\left(\frac{\Delta K_{\text{th(l)}}^R}{\Delta\sigma_{\text{w}}^R}\right)^2\right\}^{0.5}} \quad (3)$$

The dependence of $\Delta\sigma_w^R$ on the stress ratio was obtained from modified Goodman Eq. (4).

$$\sigma_a = \sigma_w\left(1-\frac{\sigma_m}{\sigma_B}\right) \quad (4)$$

Where σ_a, σ_w, σ_m, and σ_B is stress amplitude, fatigue limit of R=-1, mean stress and tensile strength, respectively.

The dependence of $\Delta K_{th(l)}^R$ on the stress ratio was obtained from Eq. (5).

$$\Delta K_{th(l)}^R = \Delta K_{th(l)}^R\sqrt{(1-R} \quad (5)$$

3. Specimen and Properties of Material

The material used in this study is the offshore structural steel F690. Table 1 shows the chemical compositions and mechanical properties of F690. Fatigue tests were conducted with four-point bending at the stress ratio (R = 0.1). Fig. 1 shows the shape of the specimen, and a schematic of the four-point bending load, with lower span of 150 mm, and upper span of 20 mm. The fatigue limit (σ_w^R) obtained at the stress ratio (R = 0.1) is 740 MPa, and the threshold stress intensity factor ($K_{th(l)}^R$) is 6.51 MPa$\sqrt{m}$ obtained at 1TCT with a thickness of 12.5 mm.

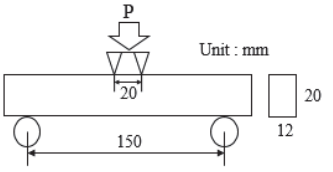

Fig. 1 Shape of specimen, and schematic of four-point bending

4. Evaluation Results and Discussion

The aspect ratio (As) was made into three types of (1.0, 0.6, and 0.4). The stress ratio

Table 1. Chemical compositions (wt.%) and mechanical properties of F690

C	Si	Mn	P	S	Al	N	Nb	V	Ti	B
0.18	0.46	1.6	0.025	0.025	0.045	0.02	0.038	0.03	0.02	0.005

Yield strength (MPa)	Tensile strength (MPa)	Elongation (%)	Hardness (HV)
851	876	15.2	553.8

(R) was set to (0.0, 0.1, and 0.5). σ_w^R and $K_{th(l)}^R$ according to the stress ratio were obtained from Eqs. (4) and (5) using the result of R = 0.1 obtained in the experiment. Table 2 shows σ_w^R and $K_{th(l)}^R$ according to the stress ratio:

Table 2. Data of F690 for the evaluation of K_{th}^R

$2b$ (mm)	t (mm)	As (a/c)	R	σ_w^R (MPa)	$K_{th(l)}^R$ (MPa · m$^{0.5}$)
12	20	1.0, 0.6, 0.4	0.0	775.5	6.86
			0.1	740.0	6.51
			0.5	541.8	4.85

The results of Table 1 were used to evaluate $K_{th(s)}^R$ and σ_{wc}^R according to the crack size. The Ando and Tange equations (Eqs. (2) and (3), respectively), were used for evaluation.

Fig. 2 shows the crack depth dependence of $K_{th(s)}^R$. Fig. 2 (a), (b), and (c) evaluate $K_{th(s)}^R$ according to the stress ratio (R) of As = (1.0, 0.6, and 0.4), respectively. $K_{th(s)}^R$ depends on the crack depth, and as the crack grows, increases. The convergence value is $K_{th(l)}^R$. The crack depth satisfying $K_{th(l)}^R$ is highly dependent on the crack shape. The larger the $K_{th(l)}^R$ and σ_w^R of the material, the shorter the crack depth at which $\Delta K_{th(s)}^R$ converges to $\Delta K_{th(l)}^R$. Table 3 shows five crack depths by the Tange and Ando equations. The table shows that $\Delta K_{th(s)}^R$ was almost similar, regardless of the stress ratio (R) and aspect ratio (As). Therefore, hereinafter, $\Delta K_{th(s)}^R$ by the Ando equation will be described. In the case of As

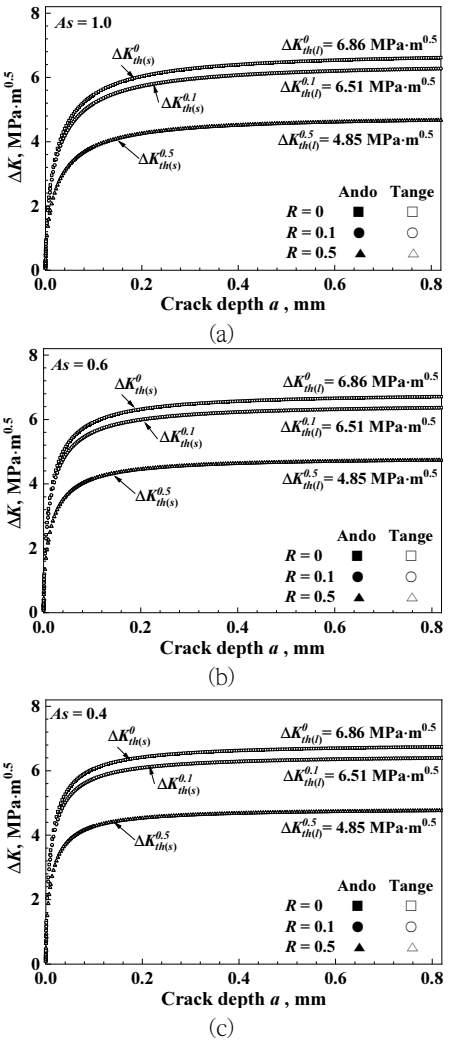

Fig. 2 Threshold stress intensity factor ($\Delta K_{th(s)}^R$) depending on crack depth. (a) As = 1.0, (b) As = 0.6, and (c) As = 0.4

= (1.0, 0.6, and 0.4), it can be seen that as the crack depth increases, the stress ratio R = (0, 0.1, and 0.5) converges to each $\Delta K_{th(l)}^R$. For $\Delta K_{th(s)}^R$, the smaller As was found to converge faster at $\Delta K_{th(l)}^R$ = 6.86 MPa$\sqrt{m}$. That is, when compared at the stress ratio (R = 0) and the

Table 3. Threshold stress intensity factor ($\Delta K^R_{th(s)}$) for each crack depth depending on the stress ratio and aspect ratio (unit: MPa$\sqrt{m}$)

a(mm) \ R	0.0		0.1		0.5	
	Ando	Tange	Ando	Tange	Ando	Tange
As = 1.0						
0.01	2.65	2.65	2.53	2.53	2.00	2.00
0.04	4.39	4.40	4.18	4.19	3.08	3.09
0.5	6.47	6.48	6.14	6.15	4.57	4.58
1.0	6.65	6.65	6.31	6.31	4.70	4.70
3.0	6.79	6.44	6.44	6.44	4.80	4.80
As = 0.6						
0.01	3.22	3.23	3.07	3.08	2.26	2.26
0.04	4.98	5.00	4.74	4.76	3.50	3.52
0.5	6.61	6.62	6.28	6.28	4.67	4.68
1.0	6.73	6.73	6.39	6.39	4.76	4.76
3.0	6.83	6.83	6.48	6.48	4.83	4.83
As = 0.4						
0.01	3.53	3.54	3.36	3.37	2.47	2.48
0.04	5.26	5.27	5.00	5.01	3.70	3.71
0.5	6.67	6.67	6.33	6.33	4.71	4.71
1.0	6.76	6.76	6.42	6.42	4.78	4.78
3.0	6.84	6.84	6.49	6.49	4.84	4.84

crack depth a = 3.0 mm, As = 1.0 is $\Delta K^R_{th(s)}$ = 6.79 MPa$\sqrt{m}$, As = 0.6 MPa$\sqrt{m}$ is $\Delta K^R_{th(s)}$ = 6.83 MPa$\sqrt{m}$, and As = 0.4 is $\Delta K^R_{th(s)}$ = 6.84 MPa$\sqrt{m}$. In addition, the $\Delta K^R_{th(s)}$ of the crack depth a = 0.04 mm is 4.39 MPa$\sqrt{m}$ (As = 1.0), 4.98 MPa$\sqrt{m}$ (As = 0.6), and 5.26 MPa$\sqrt{m}$ (As = 0.4), respectively, indicating that the $\Delta K^R_{th(s)}$ for the smaller As was larger. This is because when the surface length is larger than the depth, the crack propagation is faster in the depth direction.

Fig. 3 shows the dependence of $\Delta\sigma^R_{wc}$ on the crack depth. Fig. 3 (a), (b) and (c) evaluate

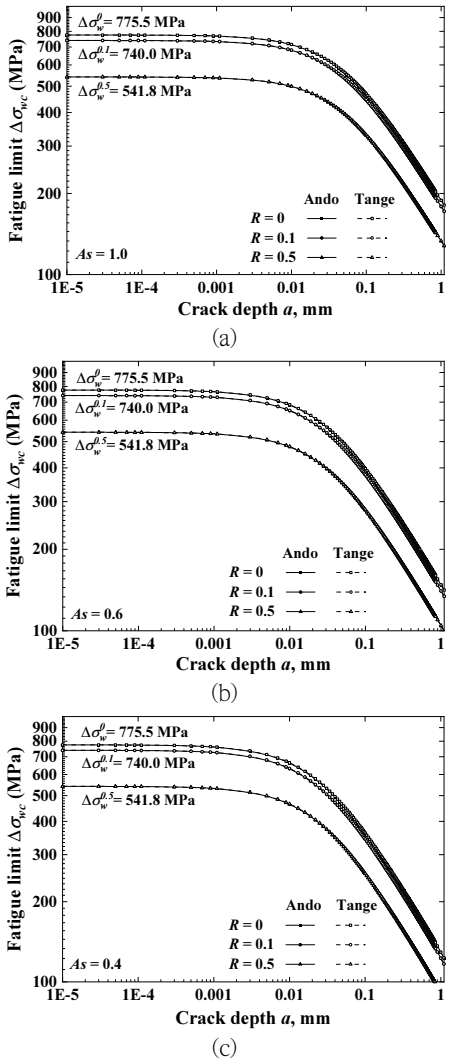

Fig. 3 Fatigue limit ($\Delta\sigma^R_{wc}$) depending on crack depth (a) As = 1.0, (b) As = 0.6, and (c) As = 0.4

$\Delta\sigma^R_{wc}$ according to the stress ratio (R) of As = (1.0, 0.6 and 0.4), respectively. $\Delta\sigma^R_{wc}$ depends on the crack size, and as the crack grows, decreases. Table 4 shows the $\Delta\sigma^R_{wc}$ by the Tange and Ando equations for the five crack depths. The $\Delta\sigma^R_{wc}$ values are almost similar, regardless of the stress ratio (R) and the

Table 4. Fatigue limit ($\Delta\sigma_{wc}^{R}$) for each crack depth depending on the stress ratio (R) and aspect ratio (As) (unit: MPa$\sqrt{m}$)

a(mm) \ R	0.0		0.1		0.5	
	Ando	Tange	Ando	Tange	Ando	Tange
As = 1.0						
0.01	714	715	680	682	500	501
0.04	592	595	564	566	416	417
0.5	254	254	241	241	179	179
1.0	189	189	179	179	133	133
3.0	111	111	105	105	78	78
As = 0.6						
0.01	682	684	650	652	478	479
0.04	529	531	503	505	372	373
0.5	203	203	193	193	143	143
1.0	148	148	140	140	104	104
3.0	74	74	70	70	53	53
As = 0.4						
0.01	662	664	631	633	464	466
0.04	494	496	470	472	348	349
0.5	181	181	171	171	128	128
1.0	129	129	123	123	91	91
3.0	51	51	48	48	36	36

aspect ratio (As). Therefore, hereinafter, $\Delta\sigma_{wc}^{R}$ by the Ando equation will be described. The $\Delta\sigma_{wc}^{R}$ of the cracked material decreases by approximately 8 % (As = 1.0), 12 % (As = 0.6), and 15 % (As = 0.4) at the crack depth a = 0.01 mm, regardless of the stress ratio (R), and then rapidly decreases. The abruptly decreasing slope corresponds to the threshold stress intensity factor $\Delta K_{th(l)}^{R}$ of a large crack. The crack depth a = 3 mm decreases approximately 86 % (As = 1.0), 92 % (As = 0.6), and 93 % (As = 0.4). At the same aspect ratio (As), as the stress ratio (R) increase, $\Delta\sigma_{wc}^{R}$ gets smaller. This is because the increase of the stress ratio (R) increases the average stress, so that the crack propagation rate increases. In addition, the smaller the As, the smaller the fatigue limit ($\Delta\sigma_{wc}^{R}$). This is because the crack propagation of the depth direction increases. Therefore, since the fatigue limit depends on the stress ratio (R) and aspect ratio (As), it is necessary to pay attention to the crack control of the structure by nondestructive inspection.

The crack dimension dependencies of $\Delta\sigma_{wc}^{R}$ and $\Delta K_{th(s)}^{R}$ obtained from Eqs. (1) and (2) agree very well. The two equations agree very well, regardless of the aspect ratio (As) and the stress ratio (R). From this result, the fatigue limit of the El Haddad research can be evaluated by the Ando Eq. (2). El Haddad et al. induced an evaluation equation of $\Delta K_{th(s)}^{R}$ depending on the crack length, by summing the initial crack length and the microcrack length grown by cyclic stress. On the other hand, Ando et al. induced the evaluation equation for the size of the Dugdale model plastic zone by cyclic stress, which does not depend on the crack size. Although the basic concepts and the types of equation differ, the $\Delta K_{th(s)}^{R}$ values by the Ando Eq. (2) and Tange Eq. (3) are almost the same. They are judged to have similar results, because the microcrack size due to cyclic stress or the plastic zone size of the Dugdale model satisfies the small-scale yield range.

5. Conclusions

The threshold stress intensity factor $\Delta K_{th(s)}^{R}$ and fatigue limit $\Delta\sigma_{wc}^{R}$ were evaluated according to the small crack of the offshore structural steel F690 using the Tange equation that modified the El Haddad equation, and the Ando equation that considered the plasticity area of the fatigue crack tip. Although the two equations differ in the induced concept and the shape of equation, the $\Delta K_{th(s)}^{R}$ and $\Delta\sigma_{wc}^{R}$ results of the small crack are completely consistent. These equations will therefore be able to evaluate the small crack dimensional dependence of the lower limit stress intensity factor and fatigue limit of all steel structures.

References

[1] I. Milne, R. A. Ainsworth, A. R. Dowling, A. T. Stewart, "Assessment of the integrity of structures containing defects", International Journal of Pressure Vessels and Piping, vol. 32, pp. 3-104, (1988).

[2] Y. Akita, K. Ikeda, N. Iwai, "On brittle fracture initiation. (First report – deep notch test)", Journal of The Japan Society of Naval Architects and Ocean Engineers, vol. 1964, no. 116, pp. 136-146, (1964).

[3] P. Paris, F. A. Erdogan, "A Critical analysis of crack propagation laws", Journal of Basic Engineering, vol. 85, pp. 528-533, (1963).

[4] H. L. Dunegan, A. S. Tetelman, "Non-destructive characterization of hydrogen-embrittlement cracking by acoustic emission techniques", Engineering Fracture Mechanics, vol. 2, pp. 387-402, (1971).

[5] ASME B&PV Code Section XI, "Rules for in-service inspection of nuclear power plant components", American Society of Mechanical Engineers, (2013).

[6] API 579-1/ASME FFS-1, "Recommended practice for fitness-for-service 2nd Edition", American Petroleum Institute, (2007).

[7] WES2805–1997 Codes for The Japan Welding Engineering Society, "Evaluation method for defects on brittle fracture of welded joint", The Japan Welding Engineering Society, (1997).

[8] HPIS Z 101, "Assessment procedure for crack-like flawsure equipment", High Pressure Institute of Japan, (2008).

[9] JSME SNAI-2017, "Codes for nuclear power generation facilities – Rules on fitness-for-service for nuclear power plants", The Japan Society of Mechanical Engineers, (2017).

[10] W. F. Brown, A. E. Srawley, "Plane strain crack toughness testing of high strength metallic materials", ASTM STP 410, pp. 1-129, (1966).

[11] ANSI/ASTM E399-78, "Standard test method for plane strain fracture toughness of Metallic Materials", Annual Book of ASTM Standards, Part 10, American Society for Testing and Materials, (1978).

[12] M. Liu, Y. Gan, D. A. H. Hanaor, B. Liu, C. Chen, "An improved semi-analytical solution for stress at round-tip notches", Engineering Fracture Mechanics, vol. 149, pp. 134–143, (2015).

[13] R. T. Davenport, R. Brook, "The threshold stress intensity factor range in fatigue", Fatigue of Engineering Materials and Structures, vol. 1, pp. 151-158, (1979).

[14] M. H. EI Haddad, T. H. Topper, K. N. Smith, "Prediction of non-propagating cracks", Engineering Fracture Mechanics, vol. 11, pp. 573-584, (1979).

[15] A. Tange, T. Akutu, N. Takamura, "Relation between shot-peening residual stress distribution and fatigue crack propagation life in spring steel", Transactions of Japan Society for Spring Engineers, vol. 1991, no. 36, pp. 47-53, (1991).

[16] K. Ando, R. Fueki, K. W. Nam, K. Matsui, K. Takahashi, “A study on the unification of the threshold stress intensity factor for micro crack growth”, Transactions of Japan Society for Spring Engineers, vol. 2019, no. 64, pp. 39-44, (2019).
[17] D. S. Dugdale, “Yielding of steel sheets containing slits”, Journal of the Mechanics and Physics of Solids, vol. 8, pp. 100-104, (1960).
[18] W. G. Lee, K. H. Gu, C. S. Kim, K. W. Nam, “Reliability Improvement of Offshore Structural Steel F690 Using Surface Crack Nondamaging Technology”, Journal of Ocean Engineering and Technology, vol. 35, pp. 327-335, (2021).
[19] S. H. Yun, K. W. Nam, “Failure Analysis and Counter measures of SCM435 High-Tension Bolt of Three-Step Injection Mold”, Journal of The Korean Society of Industry Convergence, Vol. 23, No. 4, pp. 531-539, (2020).

Manuscript received February 3, 2022;
revised February 22, 2022; accepted February 28, 2022